Uniform quasi-convex optimisation via Extremum Seeking

Uniform quasi-convex optimisation via Extremum Seeking

Nicola Mimmo, Lorenzo Marconi and Giuseppe Notarstefano

***Abstract*— The paper deals with a well-known extremum seeking scheme by proving uniformity properties with respect to the amplitudes of the dither signal and of the cost function. Those properties are then used to show that the scheme guarantees the global minimiser to be semi-global practically stable despite the presence of local saddle points. To achieve these results, we analyse the average system associated with the extremum seeking scheme via arguments based on the Fourier series.**

I. Introduction

The Extremum Seeking (ES) are algorithms being studied since early 1900 [1]. This optimisation technique has been widely applied and, among all the use cases we remember electronics [2], mechatronics [3], mechanics [4], aerodynamics [5], thermohydraulics [6], and thermoacoustic [7]. In particular, this paper analyses the ES strategies proposed in [8], [9]. These represent some of the most cited algorithms despite the literature offering several alternatives. As an example, an integral action was investigated in [10], an estimator of the cost function's parameters was proposed in [11], [12], an observer was added in [13], the use of fractional derivatives was introduced in [3], the compensation of output delays was proposed in [14], a Newton-based strategy was investigated in [15], [16], and a simplex method was added in [17].

A common feature of all the listed schemes consists of a perturbation of the plant to be optimised. This perturbation, usually called *dither*, is implemented through a periodic signal. This signal aims at discovering the search direction that reduces the cost function (as for minimisation problems). Due to the periodicity of the dither, the ES algorithms are analysed through the *averaging theory* [18]. Commonly, these analyses prove the ES algorithms are *asymptotically practically* converging to the minimiser. Besides, it also demonstrated that the *average* is a good representative of the original system, *i.e.* the trajectories of the original system and those of the averaging remain close to each other, provided that a design parameter, in this paper denoted with γ, is designed sufficiently small [19], [20], [9], [21], [22]. Roughly, γ embeds a time-scale separation between the dither period and the dynamics of the optimiser. Thus, keeping γ small means that the optimiser evolves in a time-scale much larger than the dither period.

This research was partially supported by the European Project "AerIal RoBotic technologies for professiOnal seaRch aNd rescuE" (AirBorne), Call: H2020, ICT-25-2016/17, Grant Agreement no: 780960.

The authors are with the Department of Electrical and Information Engineering, "Guglielmo Marconi", University of Bologna, 40126 Bologna, Italy, e-mail: {nicola.mimmo2, lorenzo.marconi, giuseppe.notarstefano}@unibo.it

For comprehensiveness, we cite [23], [24] that use the value of the cost function to perturb the dither's phase. These ES schemes are usually analysed via Lie-derivatives tools.

This paper presents two main contributions to the framework of the previous research context.

As the first one, the scheme proposed in [8] is re-analysed through Fourier series arguments. It results that, thanks to this different point of view, the ES scheme of [8] can be applied to quasi-convex functions, *i.e.* functions which have a unique minimiser but possess saddle points. Our studies demonstrate that, on average, the trajectories are bounded and converge to a neighbourhood of the minimiser. Besides, the width of this neighbourhood is demonstrated to be proportional to the amplitude of the dither. It is also important to note that, based on the analyses conducted in this work, the dither's amplitude is not required to be small. As for the second one, we prove that if the ES scheme of [8] is extended with a high-pass filter, the design of γ becomes uniform in the cost function's value. More in detail, the semi-global and practical stability of the minimiser is proved where the tuning parameter γ only depends on the cost's Lipschitz constant (not on the cost value).

The rest of this work consists of four sections. Section II describes the problem formulation and reviews the basic ES scheme detailed in [8]. Moreover, Section II also shows how the Fourier series can be proficiently used to extend the applicability of the ES scheme of [8] to quasi-convex cost functions. Section III aims at presenting the benefits, associated with the introduction of a high-pass filter, in terms of uniformity with respect to the value of the cost function. Section IV proposes numerical tests to corroborate the theoretical achievements while Section V concludes this work with some remarks.

This paper claims theoretical results whose proofs are detailed in [25].

II. Problem Formulation

The ES problem consists of the optimisation of an unknown cost function $h : \mathbb{R} \to \mathbb{R}$ satisfying the following two assumptions.

Assumption 1 *The function h is smooth and there exists a $x^\star \in \mathbb{R}$ such that*

$$h(x) - h(x^\star) > 0 \quad \forall\, x \in \mathbb{R} : x \neq x^\star.$$

Assumption 2 *There exist a locally Lipschitz and strictly quasi-convex function $m : \mathbb{R} \to \mathbb{R}$, a class-$\mathcal{K}_\infty$ function $\alpha(\cdot)$ such that for all $x_1, x_2 \in \mathbb{R} : (x_1 - x^\star)(x_2 - x^\star) \geq 0$*

$$|m(x_2) - m(x_1)| \geq \alpha(|x_2 - x_1|).$$

Remark 1 *As for Assumption 2, it asks for a (not necessarily strict) monotone behaviour of h, where the latter could have isolated saddle points. In other words, $h(\cdot)$ belongs to the class of the so-called strictly quasi-convex functions [26]. Assumption 2 is weaker than the common assumption $(\partial h(x)/\partial x)x > 0$ for any $x \neq x^\star$ typically present in literature, (see, among the others, [[8], Assumptions 3 and 4]) ruling out the existence of local saddle points.*

The problem of *semi-global extremum seeking* can be formulated in the following way. For any $\epsilon > 0$ and $r_0 > 0$, design a system of the form

$$\dot{x} = \varphi_{\epsilon,r_0}(x, h(x), t) \quad x(0) = x_0,$$

so that for all x_0 satisfying $|x_0 - x^\star| \leq r_0$ the resulting trajectories $x(t)$ are bounded and satisfy $\lim_{t\to\infty} \sup |x(t) - x^\star| \leq \epsilon$.

Among the different ES schemes proposed in the literature to solve the previous problem, a common one is given by (see [8])

$$\dot{x} = -\gamma\, y_\delta(x,t)\, u(t) \qquad x(0) = x_0 \tag{1}$$

in which $y_\delta(x,t) := h(x + \delta u(t))$, $u(t) := \sin(2\pi t)$ is the dither signal and $\gamma, \delta > 0$ are tunable parameters[1]. The block diagram of this algorithm is represented in Figure 2. In the next part, we briefly comment on the main properties, as available in the literature, of this algorithm and strengthen them.

Since the right-hand side of (1) is 1-periodic, the average system linked to (1) is given by ([27], §10.4)

$$\dot{x}_a = -\gamma \int_0^1 y_\delta(x_a, t) u(t) dt\,. \tag{2}$$

In the remaining part of the section, we present a different route for the analysis of (2) based on a Fourier series expansion rather than on the Taylor one used in the available literature. This analysis allows one to claim stronger results on (1).

The smoothness of $h(\cdot)$ in Assumption 1 is essentially asked to guarantee the existence of the Fourier series of the function y_δ[2]. Then, since $y_\delta(x_a, t)$ and its time derivatives are continuous and periodic, $y_\delta(x_a, t)$ can be expressed in terms of its Fourier series as

$$\begin{aligned} y_\delta(x_a,t) = \frac{a_{0,\delta}(x_a)}{2} + \\ \sum_{k=1}^{\infty} a_{k,\delta}(x_a)\cos(k2\pi t) + b_{k,\delta}(x_a)\sin(k2\pi t) \end{aligned} \tag{3}$$

where

$$\begin{aligned} a_{k,\delta}(x_a) &:= 2\int_0^1 y_\delta(x_a,t)\cos(k2\pi t)\, dt \\ b_{k,\delta}(x_a) &:= 2\int_0^1 y_\delta(x_a,t)\sin(k2\pi t)\, dt\,. \end{aligned} \tag{4}$$

[1]The general case of a dither takes the form $\tau \mapsto \sin(\omega\tau)$ with $\omega > 0$, $\tau \in \mathbb{R}$ (as considered in [8]) can be always obtained by rescaling the time as $t = \tau\, 2\pi/\omega$.

[2]Milder regularity properties guaranteeing the existence of the series could be assumed.

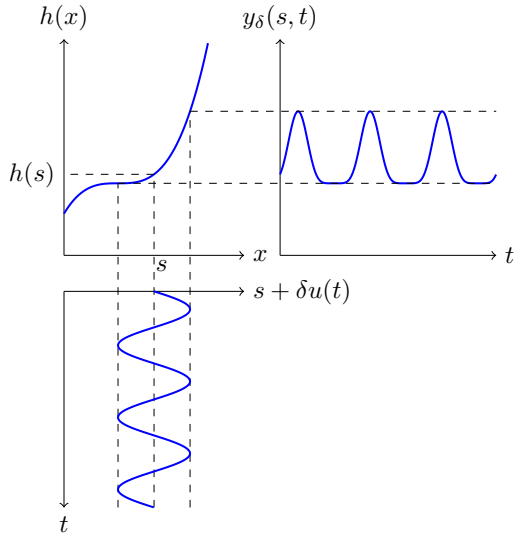

Fig. 1: Graphical representation of the periodic behaviour of $y_\delta(s,t)$. Conceiving s as a parameter, we see that the oscillation induced by $u(t)$ is elaborated by the non-linear map $h(\cdot)$ and results in a periodic function of time (top-right). This latter can be described through its Fourier coefficients $a_k(s)$ and $b_k(s)$.

Embedding (3) in (2) it is immediately seen that the average system linked to (1) reads as

$$\dot{x}_a = -\frac{\gamma}{2} b_{1,\delta}(x_a)\,. \tag{5}$$

For the system (5) the following result holds. In the result, we refer to the class-$\mathcal{K}_\infty$ function $\underline{\delta}^\star(\cdot)$ defined as

$$\underline{\delta}^\star(s) := 2\int_0^{1/2} \alpha(s\sin(2\pi t))\, dt \tag{6}$$

Lemma 1 *Let $h(\cdot)$ be such that Assumptions 1-2 are satisfied. Then:*

a) *for all positive δ there exists a compact set $\mathcal{A}_\delta \subseteq [x^\star - \delta, x^\star + \delta]$ that is globally asymptotically and locally exponentially stable for (5).*

b) *There exists a $\bar{\delta}^\star > 0$ such that, for all positive δ such that $\delta \leq \bar{\delta}^\star$, there exists an equilibrium point $x^\star_{a\delta} \in$ int $\mathcal{A}_\delta$ that is locally exponentially stable for system (5). If, in addition, the function $\bar{h}(s) := h(x^\star + s) - h(x^\star)$ is even, then $x^\star_{a\delta} = x^\star$.*

Item a) of the previous lemma states that the trajectories of the average system reach a compact set $\mathcal{A}_\delta$ that is contained in a δ neighbourhood of $x^\star$ for all possible δ. This, in particular, implies that there exists a class $\mathcal{KL}$ function $\beta(\cdot,\cdot) : \mathbb{R} \times \mathbb{R}_+ \to \mathbb{R}_+$ such that

$$|x_a(t)|_{\mathcal{A}_\delta} \leq \beta(|x_a(0)|_{\mathcal{A}_\delta}, t)$$

where $|\cdot|_{\mathcal{A}_\delta}$ denotes the distance to the set $\mathcal{A}_\delta$. Item b) claims that the set $\mathcal{A}_\delta$ collapses to an equilibrium point if δ is also taken sufficiently small. Moreover, the last point of item b) shows that $x^\star$ represents the equilibrium point

only for cost functions that are locally symmetric around the optimum.

Standard averaging results can be then used to show that the same property is preserved also for the trajectories of the original system (1) for sufficiently small γ but in a semi-global and practical way. This is detailed in the next Proposition 1 where we refer to the class $\mathcal{K}_\infty$ function $\chi(s)$ defined as

$$\chi(s) := \beta^{-1}(s, 0).$$

In the following analysis we denote by $L_r > 0$ and $M_r > 0$, respectively the local Lipschitz constant and the upper bound of the function $h(\cdot)$ on a closed interval of length r. In particular, regularity of h implies that

- for all $r > 0$ there exists $L_r > 0$ such that for all $x_1, x_2 \in [x^\star - r,\, x^\star + r]$

$$|h(x_1) - h(x_2)| \leq L_r |x_1 - x_2| \,. \tag{7}$$

- for all $r > 0$, there exists $M_r > 0$ such that for all $x \in [x^\star - r,\, x^\star + r]$

$$|h(x)| \leq M_r \,. \tag{8}$$

Proposition 1 *Let $h(\cdot)$ be such that Assumptions 1-2 hold and let r, δ, d be arbitrary positive numbers such that $r - d - 2\delta > 0$. Let $r_0 := \chi(r - d - 2\delta)$. There exist $\bar{t}(r_0, d)$ and $\gamma^\star(M_r, L_r, \delta, d) > 0$ such that for any $\gamma \in (0,\, \gamma^\star)$, any $x_0 \in \mathbb{R} : |x_0 - x^\star| \leq r_0$, the trajectories of* (1) *are bounded and*

$$|x(t)|_{\mathcal{A}_\delta} \leq d \qquad \forall\, t \geq \frac{\bar{t}}{\gamma} \,.$$

An immediate consequence of the previous result is the next corollary showing that under Assumptions 1-2 system (1) solves the problem of semi-global extremum seeking formulated before.

Corollary 1 *Let $h(\cdot)$ be such that Assumptions 1-2 are fulfilled and let r_0 and ϵ be arbitrary positive numbers. Then, there exist $\bar{t}(r_0, \epsilon) > 0$, $\bar{\delta}^\star(\epsilon) > 0$ and $\gamma^\star(r_0, \bar{\delta}^\star, \epsilon) > 0$ such that for any $\delta \in (0, \bar{\delta}^\star)$, any $\gamma \in (0,\, \gamma^\star)$ and any $x_0 \in \mathbb{R} : |x_0 - x^\star| \leq r_0$, the trajectories of* (1) *are bounded and*

$$|x(t) - x^\star| \leq \epsilon \qquad \forall\, t \geq \frac{\bar{t}}{\gamma} \,.$$

By going through the proof of Proposition 1, it is immediately seen that $\gamma^\star$ is inversely proportional to M_r. As a consequence, the higher the cost function is within the set where $x(t)$ ranges, the lower the value of γ and, in turn, the slower the convergence rate of x to the neighbourhood of the optimum. Section III presents an improvement of (1) overtaking this limitation.

A. Comments on Taylor expansion-based averaging analyses

The analysis of (2) is typically approached, see [8], by using a Taylor expansion of $h(\cdot)$ to obtain a system of the form

$$\dot{x}_a = -\gamma c_1 \delta \left.\frac{\partial h}{\partial x}\right|_{x_a} - \gamma \sum_{k=2}^{\infty} c_k\, \delta^{2k-1} \left.\frac{\partial^{2k-1} h}{\partial x^{2k-1}}\right|_{x_a} \tag{9}$$

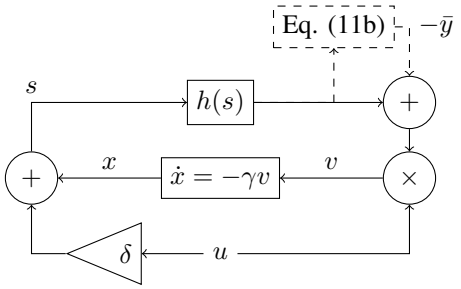

Fig. 2: The HPF-ES scheme consists of an extension of the classic ES algorithm with the addition of the dashed block.

where c_k are suitably defined positive coefficients. A key role in the study of this system is played by the first-order approximation

$$\dot{x}_a \approx -\gamma c_1 \delta \left.\frac{\partial h}{\partial x}\right|_{x_a} . \tag{10}$$

Remark 2 *The adoption of Fourier series arguments leads to* (5) *which is an exact representation of the dynamics of the average, uniform in δ. On the opposite,* (10) *represents an approximation that deteriorates as δ becomes larger.*

Note that, if our Assumption 2 is strengthen by asking that, for any $x \neq x^\star$, it holds $(\partial h(x)/\partial x)(x - x^\star) > 0$ (respectively $> \alpha(|x - x^\star|)$ with $\alpha(\cdot)$ a class-$\mathcal{K}$ function, see [8], Assumptions 3 and 4), then the Lyapunov arguments of [[8], eq. (45)] demonstrate $x^\star$ to be a stable (respectively globally asymptotically stable) equilibrium point for (10). These stability properties are transferred to (2) for sufficiently small δ. Then, averaging techniques [27] can be used to prove that, for sufficiently small γ, the trajectories of (1) and (2) remain arbitrarily close. Namely, the semi-global extremum seeking problem is solved.

The fact that the asymptotic properties of the average system (2) are just ensured by the first-order term (10), and thus by the gradient of h, implies that isolated local saddle points, of h, cannot be handled by that proof technique. This justifies why [[8], Assumption 3], which is stronger than our Assumption 2, is needed. Furthermore, we observe that the previous analysis requires that the dither amplitude is kept sufficiently small for the higher-order terms of the average dynamics to be negligible.

III. The High-Pass Filter (HPF)-ES Algorithm

In [8] the authors proposed the next modification of (1)

$$\dot{x} = -\gamma\, (y_\delta(x,t) - \bar{y})\; u(t) \qquad x(0) = x_0 \tag{11a}$$

$$\dot{\bar{y}} = \gamma\, (y_\delta(x,t) - \bar{y}) \qquad \bar{y}(0) = \bar{y}_0 \tag{11b}$$

where $u(t)$ is the dither signal defined before, and $(x, \bar{y}) \in \mathbb{R} \times \mathbb{R}$. A block representation of (11) is depicted in Figure 2.

The intuition behind the previous scheme is to interpret $y_\delta(x,t) - \bar{y}$ as the output of a high pass filter of y_δ. Moreover, the difference $y_\delta(x,t) - \bar{y}$ represents a sort of *weighted* local variation of $h(\cdot)$ around x, directly proportional to a *weighted*

local Lipschitz constant. In the following, we show how this feature guarantees that the upper bound for the value of γ is not dependent on M_r (eq. (8)) but rather only on L_r ((7)). As for γ, similarly to (1), it must be small to let x and $\bar{y}$ be sufficiently slow to preserve the correlation between the oscillations of $y_\delta(x,t) - \bar{y}$ and those of $u(t)$. The average system of (11) is defined as

$$\dot{x}_a = -\gamma \int_0^1 \left(y_\delta(x_a,\tau) - \bar{y}_a\right) u(\tau)\, d\tau \tag{12a}$$

$$\dot{\bar{y}}_a = -\gamma\, \bar{y}_a + \gamma \int_0^1 y_\delta(x_a,\tau)\, d\tau. \tag{12b}$$

By expanding $y_\delta(x_a,t)$ in terms of the Fourier series as in the previous section, it turns out that

$$\int_0^1 y_\delta(x_a,\tau)\, d\tau = \frac{a_{0,\delta}(x_a)}{2} \tag{13a}$$

$$\int_0^1 \left(y_\delta(x_a,\tau) - \bar{y}_a\right) u(\tau)\, d\tau = \frac{b_{1,\delta}(x_a)}{2} \tag{13b}$$

where in the latter we exploited $\int_0^1 \bar{y}_a u(\tau) d\tau = 0$ and (4).

Hence, the average system reads as

$$\dot{x}_a = -\gamma \frac{b_{1,\delta}(x_a)}{2} \tag{14a}$$

$$\dot{\bar{y}}_a = -\gamma\, \bar{y}_a + \gamma\, \frac{a_{0,\delta}(x_a)}{2} \tag{14b}$$

which is a cascade where the first subsystem coincides with (5) and the second subsystem is linear and asymptotically stable. From this, the next result follows from Lemma 1.

Lemma 2 *Let $h(\cdot)$ be such that Assumptions 1-2 are satisfied. Then:*

a) *for any positive $\delta > 0$ there exist a compact set $\mathcal{A}_\delta \subseteq [x^\star - \delta, x^\star + \delta]$ and a continuous function $\tau : \mathbb{R} \to \mathbb{R}$ such that the set*

$$\text{graph } \tau|_{\mathcal{A}_\delta} = \{(x_a, y_a) \in \mathcal{A}_\delta \times \mathbb{R} \;:\; y_a = \tau(x_a)\}$$

is globally asymptotically and locally exponentially stable for (14).

b) *There exists $\bar{\delta}^\star > 0$ such that, for any $\delta \in (0, \bar{\delta}^\star)$, there exists an equilibrium point $(x^\star_{a\delta}, \bar{y}^\star_{a\delta}) \in \text{graph } \tau|_{\mathcal{A}_\delta}$ that is globally asymptotically and locally exponentially stable for system (5). If, in addition, the function $\bar{h}(s) := h(x^\star + s) - h(x^\star)$ is even, then $x^\star_{a\delta} = x^\star$.*

From this, the following result mimics the one of Proposition 1 with the remarkable difference that the upper bound $\gamma^\star$ of γ is uniform with respect to M_r.

Theorem 1 *Let $h(\cdot)$ be such that Assumptions 1-2 are fulfilled and let r, δ, d be arbitrary positive numbers such that $r - d - 2\delta > 0$. Let $r_0 := \chi(r - d - 2\delta)$. There exist $\bar{t}(r_0, d)$ and $\gamma^\star(L_r, \delta, d) > 0$ such that for any $\gamma \in (0, \gamma^\star)$ and any $(x_0, \bar{y}_0)$ fulfilling $|x_0 - x^\star| \le r_0$ and $|\bar{y}_0 - a_{0,\delta}(x_0)/2| \le \gamma^\star$, then the trajectories of* (11) *are bounded and*

$$\|(x(t), \bar{y}(t))\|_{\text{graph}\, \tau|_{\mathcal{A}_\delta}} \le d \qquad \forall\, t \ge \frac{\bar{t}}{\gamma}.$$

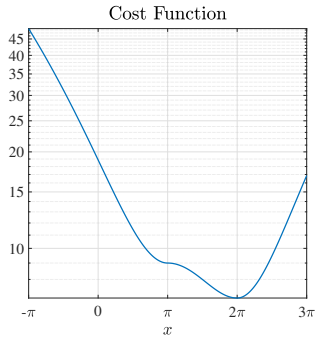

Fig. 3: Cost function (15) for $h_0 = 0$. It presents multiple points with null first derivative and it is also non-symmetric around the minimiser. The saddle point is located at $x = \pi$ and the minimiser is at $x^\star = 2\pi$.

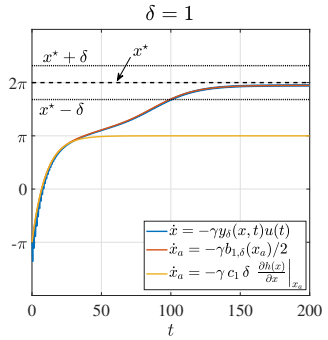

Fig. 4: The presence of saddle points stacks the Taylor-based averaging (yellow) of the classic ES (blue). Vice versa, the Fourier-based averaging (red) better represents the actual behaviour of the classic ES (blue). These results are obtained for $h_0 = 0$ and $\gamma = 0.1$.

IV. Numerical Results

This section presents numerical results obtained adopting the following cost function $h(\cdot) : \mathbb{R} \to \mathbb{R}$

$$h(x) = h_0 + \begin{cases} (x-\pi)^2 - 1 & x < \pi \\ \cos(x-\pi) - 2 & x \in [\pi,\, 2\pi) \\ (x-2\pi)^2 - 3 & x \ge 2\pi \end{cases} \tag{15}$$

where $h_0 \in \mathbb{R}$. This function, which verifies Assumptions 1 and 2, is depicted in Figure 3 for $h_0 = 10$, on $[-\pi,\, 3\pi]$.

Figure 4 reports the numerical test that shows how the ES scheme of [8] can pass over saddle points. This test also confirms that the average model (5), obtained via the Fourier series, represents the dynamics of (1) better than the first-order Taylor approximation (10).

Figures 5 and 6 show that the asymmetry of $h(\cdot)$ in the neighbourhood of $x^\star$ implies that the equilibrium point of (2) does not correspond to $x^\star$ as wrongly assessed by the averaging through Taylor expansion, see yellow lines in Figures 5 and 6. Vice versa, Figures 5 and 6 show that the trajectory of (5) (red) tracks, better than those of (10) (yellow), the trajectory of (1) (blue) and, as claimed in Lemma 1, converges into a 2δ-wide set centred at $x^\star$. The second test is performed to show that the classic ES suffers

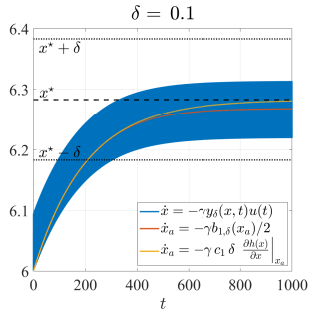

Fig. 5: The average of the classic ES, based on the Fourier series (red), converges to an equilibrium point within the set $[x^\star - \delta,\, x^\star + \delta]$ accordingly to what is foreseen in Lemma 1. Thus, the smaller is δ the closer the equilibrium point is to $x^\star$. These results are obtained for $h_0 = 10$ and $\gamma = 0.1$.

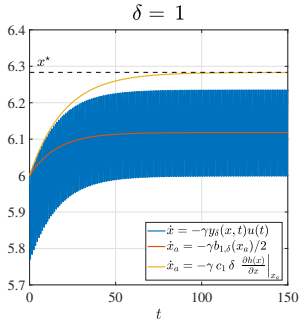

Fig. 6: The average based on the Taylor expansion (yellow) wrongly assesses $x^\star$ as an equilibrium point. Indeed, due to the asymmetry of $h(\cdot)$ around $x^\star$, the classic ES (blue) converges, on average, to an equilibrium point different from $x^\star$. Moreover, the average based on the Fourier series (red) tracks the classic ES more accurately than the first-order Taylor expansion (yellow). These results are obtained for $h_0 = 10$ and $\gamma = 1$.

of large values of $|h(\cdot)|$. Indeed, as depicted in Figure 7 (blue lines in subplots (a) and (c)), while keeping γ fixed, larger M_r lead to more oscillatory behaviours. To mathematically support this result we observe that

$$h(x + \delta u) = h(x) + R(x, \delta u) \tag{16}$$

where $R(\cdot,\cdot)$ represents the remainder of the Taylor expansion around x of $h(\cdot)$. Exploit the definition of the Lipschitz constant of $h(\cdot)$ and $|u(t)|_\infty \leq 1$ to bound the remainder from above as

$$|h(x + \delta u) - h(x)| = |R(x, \delta u)| \leq L_r \delta. \tag{17}$$

Substitute (16) into (1)

$$\dot{x} = -\gamma h(x + \delta u)u = -\gamma(h(x) + R(x, \delta u))u \tag{18}$$

and investigate the following support system

$$\dot{x}_1 = -\gamma h(x_1)u \qquad x(0) = x_{10} \tag{19}$$

conceivable as approximation of (18) for $|h(x)| \gg L_r\delta$. Let $H(x) := \int h(x)^{-1} dx$ and solve (19) by parts as

$$x_1(t) = H^{-1}(H(x_{10}) - \gamma(\cos(t) - 1)) \tag{20}$$

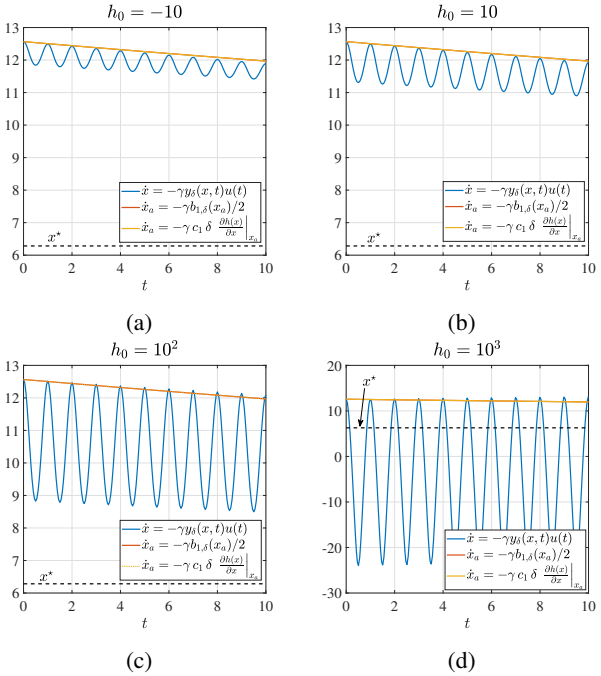

Fig. 7: The behaviour of the classic ES changes for increasing M_r. In these simulations the value of h_0 is increased from -10 to 10^3 (subplots from (a) to (d)) demonstrating that, keeping fixed γ, the classic ES (blue) becomes oscillatory for large values of the cost function. These simulations are performed with $\gamma = \delta = 0.1$.

which is a pure oscillation whose amplitude is proportional to $|H(x_{10})|$, evident in subplot (c) of Figure 7.

The third group of simulations, reported in Figure 8, shows the performance of the HPF-ES scheme whose main feature consists of better convergence performance in case of large cost functions.

Through the proposed simulations we confirm three results: a) the classic ES is able to deal with cost functions with local saddle points where, at the opposite, the average of the classic ES obtained through the Taylor expansion gets stacked (Figure 4); b) the classic ES and its average via Taylor expansion do not converge to the same equilibrium point (Figures 5 and 6); c) in case of large cost functions the classic ES behaves as an oscillator whose amplitude is proportional to the value of the cost function (Figure 7(d)). Vice versa, the adoption of the high-pass filter makes the basic ES convergence rate uniform with respect to the amplitude of the cost function.

V. Conclusions

This paper deals with two well-known extremum seeking schemes to show that they work under less restrictive assumptions. Relying on averaging and Fourier-series arguments, it is demonstrated that these schemes can deal with strictly quasi-convex cost functions making the global minimiser (assumed to be unique) semi-global practically stable. Moreover, it is shown that the presence of a high-pass filter elaborating the cost function makes the tuning of

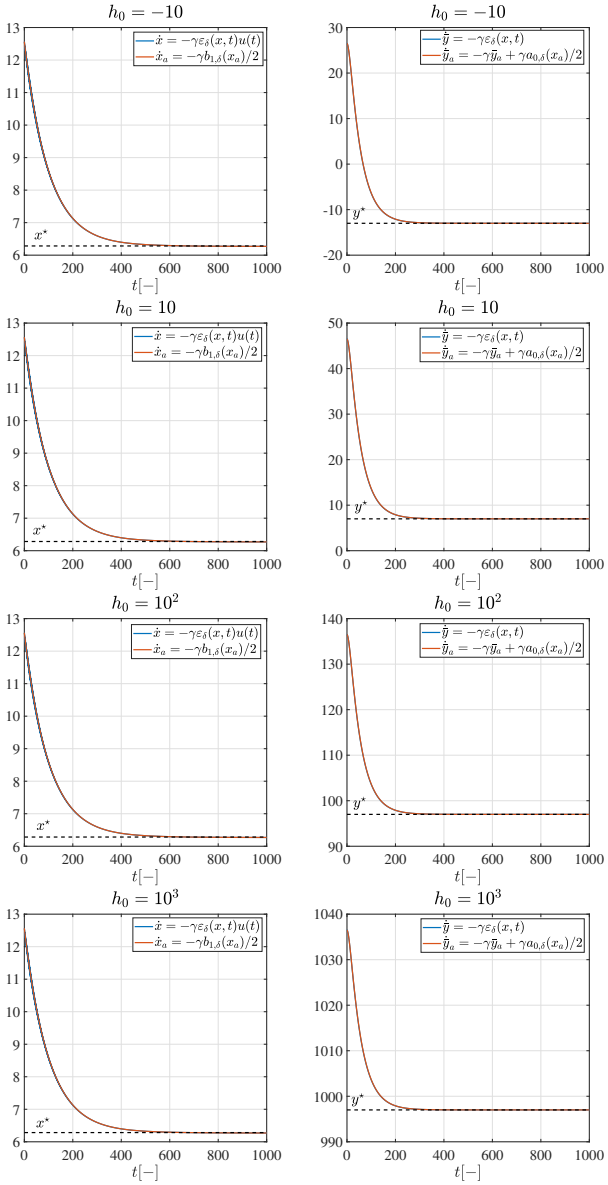

Fig. 8: The behaviour of the HPF-ES does not change for increasing M_r. In these simulations the value of h_0 is increased from -10 to 10^3 demonstrating that, keeping fixed γ, the HPF-ES keeps the same speed of convergence. These simulations are performed with $\gamma = \delta = 0.1$. (left) Behaviour of x and x_a. (right) Behaviour of $\bar{y}$ and $\bar{y}_a$.

the parameters independent of the cost magnitude.

REFERENCES

[1] D. Dochain, M. Perrier, and M. Guay, "Extremum seeking control and its application to process and reaction systems: A survey," *Mathematics and Computers in Simulation*, vol. 82, no. 3, pp. 369 – 380, 2011. 6th Vienna International Conference on Mathematical Modelling.

[2] S. F. Toloue and M. Moallem, "Multivariable sliding-mode extremum seeking control with application to mppt of an alternator-based energy conversion system," *IEEE Transactions on Industrial Electronics*, vol. 64, no. 8, pp. 6383–6391, 2017.

[3] H. Malek and Y. Chen, "Fractional order extremum seeking control: Performance and stability analysis," *IEEE/ASME Transactions on Mechatronics*, vol. 21, no. 3, pp. 1620–1628, 2016.

[4] C. Zhang and R. Ordonez, "Numerical optimization-based extremum seeking control with application to abs design," *IEEE Transactions on Automatic Control*, vol. 52, no. 3, pp. 454–467, 2007.

[5] Hsin-Hsiung Wang, S. Yeung, and M. Krstic, "Experimental application of extremum seeking on an axial-flow compressor," *IEEE Transactions on Control Systems Technology*, vol. 8, no. 2, pp. 300–309, 2000.

[6] D. J. Burns, C. R. Laughman, and M. Guay, "Proportional–integral extremum seeking for vapor compression systems," *IEEE Transactions on Control Systems Technology*, vol. 28, no. 2, pp. 403–412, 2020.

[7] W. H. Moase, C. Manzie, and M. J. Brear, "Newton-like extremum-seeking for the control of thermoacoustic instability," *IEEE Transactions on Automatic Control*, vol. 55, no. 9, pp. 2094–2105, 2010.

[8] Y. Tan, D. Nešić, and I. Mareels, "On non-local stability properties of extremum seeking control," *Automatica*, vol. 42, no. 6, pp. 889–903, 2006.

[9] M. Krstić and H.-H. Wang, "Stability of extremum seeking feedback for general nonlinear dynamic systems," *Automatica*, vol. 36, no. 4, pp. 595 – 601, 2000.

[10] M. Guay, "A perturbation-based proportional integral extremum-seeking control approach," *IEEE Transactions on Automatic Control*, vol. 61, no. 11, pp. 3370–3381, 2016.

[11] M. Guay and D. Dochain, "A minmax extremum-seeking controller design technique," *IEEE Transactions on Automatic Control*, vol. 59, no. 7, pp. 1874–1886, 2014.

[12] D. Nesic, A. Mohammadi, and C. Manzie, "A framework for extremum seeking control of systems with parameter uncertainties," *IEEE Transactions on Automatic Control*, vol. 58, no. 2, pp. 435–448, 2013.

[13] L. Hazeleger, M. Haring, and N. van de Wouw, "Extremum-seeking control for optimization of time-varying steady-state responses of nonlinear systems," *Automatica*, vol. 119, p. 109068, 2020.

[14] T. R. Oliveira, M. Krstić, and D. Tsubakino, "Extremum seeking for static maps with delays," *IEEE Transactions on Automatic Control*, vol. 62, no. 4, pp. 1911–1926, 2017.

[15] C. Labar, E. Garone, M. Kinnaert, and C. Ebenbauer, "Newton-based extremum seeking: A second-order lie bracket approximation approach," *Automatica*, vol. 105, pp. 356–367, 2019.

[16] T. R. Oliveira, J. Feiling, S. Koga, and M. Krstić, "Multivariable extremum seeking for pde dynamic systems," *IEEE Transactions on Automatic Control*, vol. 65, no. 11, pp. 4949–4956, 2020.

[17] Y. Zhang, M. Rotea, and N. Gans, "Simplex guided extremum seeking control with convergence detection to improve global performance," *IEEE Transactions on Control Systems Technology*, vol. 24, no. 4, pp. 1266–1278, 2016.

[18] F. V. J.A. Sanders, *Averaging Methods in Nonlinear Dynamical Systems*. Applied Mathematical Sciences, Springer-Verlag, 1985.

[19] A. Teel, L. Moreau, and D. Nesic, "A unified framework for input-to-state stability in systems with two time scales," *IEEE Transactions on Automatic Control*, vol. 48, no. 9, pp. 1526–1544, 2003.

[20] Y. Tan, D. Nešić, and I. Mareels, "On non-local stability properties of extremum seeking control," *IFAC Proceedings Volumes*, vol. 38, no. 1, pp. 550 – 555, 2005. 16th IFAC World Congress.

[21] A. Teel and D. Nešić, "Averaging with disturbances and closeness of solutions," *Systems & Control Letters*, vol. 40, no. 5, pp. 317 – 323, 2000.

[22] A. R. Teel, J. Peuteman, and D. Aeyels, "Semi-global practical asymptotic stability and averaging," *Systems & Control Letters*, vol. 37, no. 5, pp. 329 – 334, 1999.

[23] A. Scheinker and M. Krstić, "Extremum seeking with bounded update rates," *Systems & Control Letters*, vol. 63, pp. 25–31, 2014.

[24] Y. Zhu and E. Fridman, "Extremum seeking via a time-delay approach to averaging," *Automatica*, vol. 135, p. 109965, 2022.

[25] N. Mimmo, L. Marconi, and G. Notarstefano, "Uniform Quasi-Convex Optimisation via Exrtremum Seeking," *arXiv, https://doi.org/10.48550/arXiv.2204.00580*, 2022.

[26] S. Karamardian, "Strictly quasi-convex (concave) functions and duality in mathematical programming," *Journal of Mathematical Analysis and Applications*, vol. 20, no. 2, pp. 344–358, 1967.

[27] H. K. Khalil and J. W. Grizzle, *Nonlinear systems*, vol. 3. Prentice hall Upper Saddle River, NJ, 2002.